Microfluidics Hot Paper

International Edition: DOI: 10.1002/anie.201501794
German Edition: DOI: 10.1002/ange.201501794

Electrokinetic Size and Mobility Traps for On-site Therapeutic Drug Monitoring**

*Aliaa I. Shallan, Rosanne M. Guijt, and Michael C. Breadmore**

Abstract: *The extraction of target analytes from biological samples is a bottleneck in analysis. A microfluidic device featuring an electrokinetic size and mobility trap was formed by two nanojunctions of different pore size to extract and concentrate analytical targets from complex samples. The trap was seamlessly coupled with electrophoretic separation for quantitative analysis. The device was applied to the analysis of ampicillin levels in blood within 5 min and a linear response over the range of 2.5–20 $\mu g\,mL^{-1}$. This covers the recommended levels for treating sepsis, a critical condition with 30 to 50 % mortality and unpredicted drug levels. The device provides a new opportunity for on-site therapeutic drug monitoring, which should enable quick and accurate dosing and may save lives in such critical conditions.*

Personalized medicine promises better clinical outcomes and better global health, but socioeconomic factors hinder its wide application. Genetic testing and therapeutic drug monitoring (TDM) can be used to ensure that a patient is prescribed with the right drug at the optimum amount and dosing interval to improve efficacy and minimize toxicity. So far, most applications have been based on genetic tests. The FDA recommends genotyping before treatment with, for example, warfarin, clopidogrel, and tamoxifen. While providing valuable information, these tests fail to identify intra-patient pharmacokinetic variability that evolves as the result of a progressing disease state, drug–drug interactions, or dietary and lifestyle changes. TDM[1] uses the patient's actual drug levels to guide corrective action for any unexpected variation, especially for drugs with a narrow therapeutic window, such as antipsychotics.[2] There is also growing evidence encouraging TDM for antimicrobials in septic patients,[3] cancer drugs,[4] and immunosuppressants for organ transplants.[5] TDM is typically conducted in a laboratory setting using high-resolution separation techniques, such as liquid chromatography and electrophoresis,[6] which is not economically or logistically viable for widespread application.

Low-cost devices that can be easily operated on-site to deliver reliable data within minutes should make TDM more accessible. The most successful home tests are undoubtedly the blood glucose meter and the home pregnancy tests, which are based on biospecific recognition, using either enzymes or antibodies. While these platforms can be extended to other targets,[7] the approach is limited by the availability of a highly specific reagent for that target. This excludes the monitoring of many low-molecular-weight pharmaceuticals and their metabolites. Recently, portable electrophoretic devices were introduced for TDM of lithium[8] (under the commercial name Medimate®) and glutathione analysis.[9] These methods benefit from a high concentration of the target analyte and minimal matrix interference. For most drugs, extensive sample preparation is required to extract and concentrate the target. A recent review by Adaway and Keevil[10] illustrates that all 210 validated LC-MS/MS methods for TDM required sample treatment by solid-phase extraction, liquid–liquid extraction, or protein precipitation.

Here, we introduce electrokinetic size and mobility traps (SMTs) for the on-chip extraction, desalting, and concentration of target analytes from complex sample matrices integrated with electrophoretic separation for quantitative analysis. The SMT consists of two nanojunctions with different pore sizes connected in series to selectively extract and concentrate low-molecular-weight anions (200–1000 Da). Single nanojunctions have been reported for the concentration of DNA,[11] proteins,[12] and the extraction of pharmaceuticals from blood.[13] This is the first report of the use of nanojunctions with different pore sizes for the simultaneous extraction and concentration of target analytes from biological samples that can be seamlessly integrated with electrophoretic separation for on-site TDM.

Conceptually, an SMT exploits preferential electrokinetic transport of ions through nanochannels. When a charged surface is in contact with an electrolyte, an electric double layer (EDL) develops at the solid–liquid interface. When there is no EDL overlap, counterions with a hydrodynamic diameter smaller than the size of the nanopores can be transported, as well as co-ions smaller than the free transport region at the center of the channel. When the EDL overlaps, permselectivity develops and only counterions smaller than the nanopores will be transported by participating in the EDL leading to ion concentration polarization (ICP), where depletion and enrichment zones are generated under an applied electric field. Electrophoretic transport through the

[*] A. I. Shallan, Dr. R. M. Guijt
School of Medicine and Australian Centre for Research on Separation Science, University of Tasmania
Sandy Bay, TAS 7005 (Australia)
A. I. Shallan, Prof. M. C. Breadmore
Australian Centre for Research on Separation Science
School of Chemistry, University of Tasmania
Sandy Bay, TAS 7005 (Australia)
E-mail: mcb@utas.edu.au

[**] This work was supported by the Australian Research Council (ARC: QEII Fellowship (DP0984745) and Future Fellowship (FT130100101)). M.I.S.'s PhD scholarship is funded by the Egyptian government through the Ministry of Higher Education. R.G. acknowledges the receipt of a fellowship from the Alexander von Humboldt Foundation.

Supporting information for this article is available on the WWW under http://dx.doi.org/10.1002/anie.201501794.

nanopores also depends on the direction and magnitude of the electrophoretic mobility of the ion relative to the electroosmotic flow (EOF). The surface charge density, ionic strength inside the nanochannel, and the extent of EDL overlap determines the magnitude of the EOF, while the surface charge, positive or negative, determines its direction. Thus, the permeability of the nanojunction can be tuned to selectively transport ions within a size and mobility range.

In our device, nanojunctions were formed by dielectric breakdown,[14] the simplest and most cost-effective technique for creating a nanojunction between two microfluidic channels. While it is normally a chaotic process, we previously demonstrated control over the ion permeability by setting a current limit.[13] The precise control of the nanopore size (sub-nm) using a current limit was also reported by another group using thin insulating membranes of silicone nitride.[15] In this work, nanojunctions were created in the 100 μm wide PDMS barriers separating two V channels from a 50 μm wide central channel (Figure 1 a).

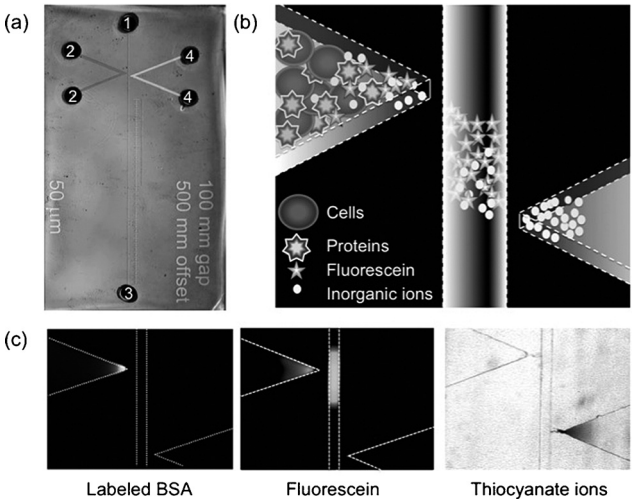

Figure 1. Electrokinetic size and mobility traps. a) Photo of the device. The separation channel connects reservoirs 1 and 3. Nanojunctions are formed in the 100 μm wide barriers between the tip of the V channels and the separation channel. Two V channels for sample (2) and waste (4) are offset by 500 μm. b) Illustration of the SMT concept. c) Microscopy images demonstrating blocking of labeled BSA (left), trapping of fluorescein (central), and transport of thiocyanate through both junctions as indicated by the formation of a complex with iron (III) (right, darker area).

The extraction nanojunction connecting the sample V channel to the separation channel was created with a 5 μA current limit to permit the passage of small ions (<1000 Da), while blocking the transport of cells, plasma proteins, and other macromolecules. The anion fluorescein (332 Da, which is similar to many pharmaceuticals) is a co-ion to the negatively charged surface, and is transported through the junction into the separation channel. This principle is applicable to most negatively charged pharmaceuticals, provided that a suitable detection method is available. The high ionic strength on both sides of the extraction junction and the use of hydroxypropyl methyl cellulose (HPMC) to shield the surface charge delays the development of ICP and allows longer injection of analyte, as shown in Figure 1 b and c.

The desalting nanojunction between the waste V channel and the separation channel was created with a 0.5 μA current limit to block the transport of target analytes, modeled by fluorescein, but allow the transport of small inorganic ions in order to desalt the sample. Together, the two nanojunctions create a trap in which molecules with a defined size/mobility range can be extracted, concentrated, and desalted (Figure 1 b).

Figure 1 c shows the behavior of the SMTs with molecules of different molecular weights. In the left panel, negatively charged bovine serum albumin (MW $\approx$ 66.5 kDa) labeled with fluorescamine is blocked based on size by the extraction nanojunction. The central panel shows fluorescein trapped in the separation channel ready for electrophoretic separation when the power supplies are switched to separation mode. The right panel shows the transport of a small inorganic anion, thiocyanate, from the sample V channel into the separation channel and then through the desalting nanojunction into the waste V channel, where it forms a complex with iron(III) (darker area). While the migration of iron into the sample V channel is also expected, the red color was not observed in the sample V channel because of the high pH value in this channel.

The matrix ionic strength and viscosity were found to affect the amount of transported ions (Figure 2 a and b). As the ionic strength and viscosity of the sample increases, ion transport quickly decreases. The SMT resulted in 100-fold enhancement over conventional pinched electrokinetic injection when the sample matrix was water (Figure 3). Two anionic fluorescent dyes with a close size/mobility ratio, fluorescein and eosin, were simultaneously injected, concentrated, then separated. This demonstrates the power of electrophoretic separation to individually detect similar analytes. The decrease in the amount of transported ions from a complex matrix was counteracted by the concentrating effect of the SMT. Whole blood samples are better suited for this method than saliva or urine, as the matrix ionic strength and viscosity are considered more consistent.

A challenging case in which TDM may become a valuable tool is dosage tailoring for critically ill septic patients. The increased volume of distribution leads to a lower concentration of hydrophilic drugs, but when the kidneys fail, decreased clearance leads to an accumulation of the drug.[16] Sepsis is fatal for 30 to 50 % of all patients.[17] Early diagnosis and quick optimization of the dosing are crucial for the patient's survival.[18] It is one of the major causes of death in newborns,[19] when both sample volume and time are critical. In a few hospitals, TDM of antimicrobials for managing sepsis is currently done using HPLC,[20] which is accurate but not accessible to all hospitals. Ampicillin is a first line antibiotic in treating sepsis and exhibits negligible binding to plasma proteins,[21] but has low stability in biological fluids,[22] making the time between sampling and analysis critical.

We used our SMT for the analysis of ampicillin in blood to demonstrate its potential for on-site TDM. Spiked whole blood samples from a healthy volunteer were labeled with

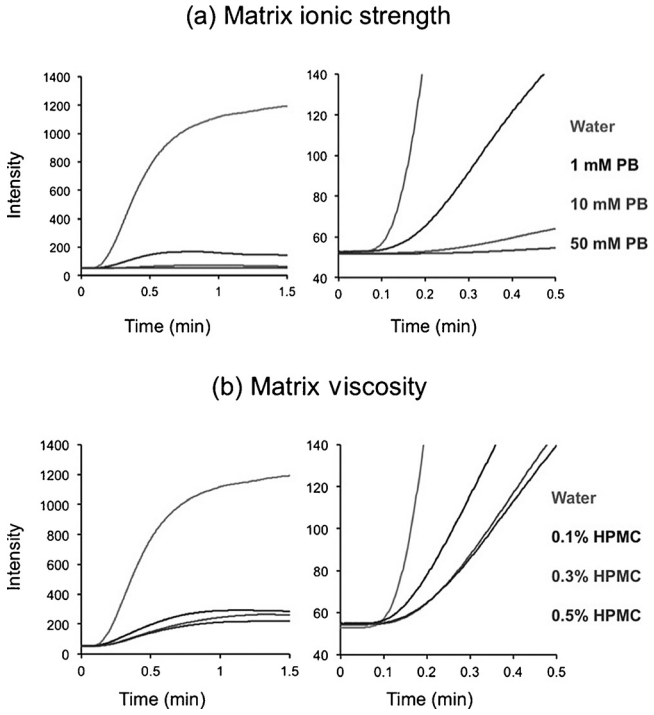

Figure 2. Fluorescence intensity at the anodic side of the extraction nanojunction as a function of injection time. Graphs on the right provide a detailed view of the early stages of enrichment. a) Effect of matrix ionic strength (top to bottom; 0, 1, 10, and 50 mM phosphate buffer, pH 11.5). b) Effect of matrix viscosity (top to bottom; 0, 0.1, 0.3, and 0.5% hydroxypropyl methyl cellulose (HPMC)). Unless stated otherwise, the sample was 0.2 ppm fluorescein in water with no HPMC, and BGE was 10 mM phosphate buffer, pH 11.0 with 0.5% HPMC. Potentials of −100, −500, −100, and +300 V were applied to reservoirs 1–4, respectively.

fluorescamine to facilitate fluorescence detection, and negative pressure was used to fill the sample V channel. Fluorescamine reacts with primary amines to produce a fluorescent compound within seconds, while the excess reagent hydrolyzes into a nonfluorescent product. Labeled ampicillin was trapped in the SMT before electrophoretic separation (Figure 4). The linear range of 2.5–20 $\mu g\,mL^{-1}$ ampicillin (relative standard deviation = RSD = 17%, $n = 4$ devices, 10 $\mu g\,mL^{-1}$ ampicillin) covers the recommended blood level for treating sepsis of 10 $\mu g\,mL^{-1}$ ampicillin. The limit of quantitation offered by HPLC methods can be as low as 0.1 $\mu g\,mL^{-1}$ using 200 µL of plasma.[23] Such low levels are not necessary, considering the minimum inhibitory concentration of ampicillin. It is more beneficial to use smaller sample volumes, especially when monitoring preterm infants, sample volume should not exceed 75 µL.[24] The proposed assay requires only 40 µL of blood to provide results within 5 min.

Here, we have introduced SMTs that function through the combination of two nanojunctions with different pore size to achieve simultaneous concentration and cleanup of small molecules from blood in a single step, and applied such

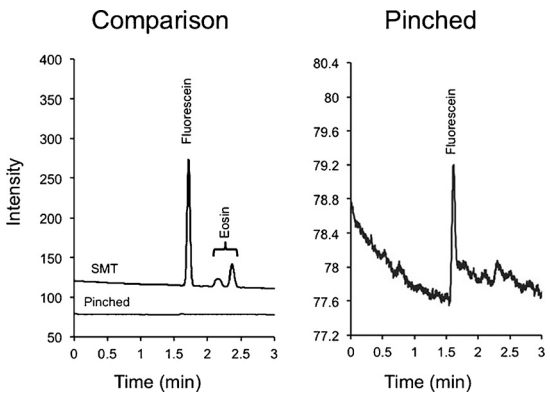

Figure 3. Electropherograms comparing SMT (top trace) with pinched injection (bottom trace and magnified right image) using 0.05 ppm fluorescein and eosin in water. SMT showed 100-fold enhancement.

a SMT to the analysis of ampicillin. Fabrication of the nanojunctions by dielectric breakdown is fast and simple, and the electronic control over the pore size allows their incorporation without significantly adding to the cost of fabrication of the microchip. The device does not rely on pumps or valves, thus allowing its simple operation. Upon further engineering of the peripherals, it is anticipated that the device will be similar in size to the medimate portable system. The ability to rapidly quantify the antibiotic ampicillin at therapeutic levels from blood within 5 min demonstrates the potential of these traps for on-site TDM. The next step will be the application of this method to clinical samples.

Experimental Section

The devices were hybrid glass/polydimethyl siloxane (PDMS) irreversibly bound after air plasma treatment. To create the nanojunctions, all channels were filled with 10 mM phosphate buffer (pH 11), and a breakdown voltage of 2200 V was applied to each V channel sequentially while keeping the separation channel grounded. The buffer used during breakdown was then replaced by the sample in the sample V channel and with the background electrolyte (BGE, 100 mM phosphate buffer, pH 11.5, and 0.5% hydroxypropyl methyl cellulose (HPMC), unless stated otherwise) in the separation channel, and with 10 mM phosphate buffer, pH 11.5, in

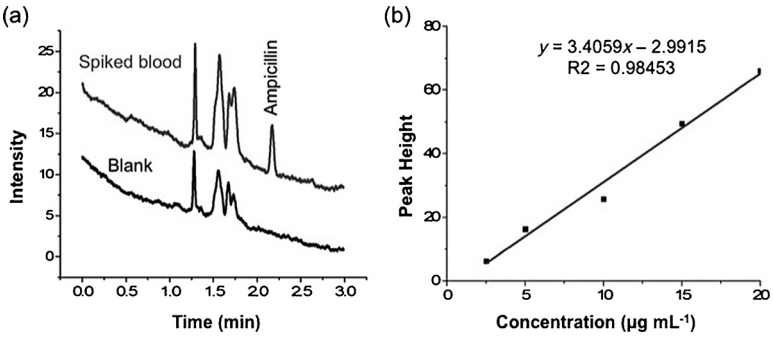

Figure 4. Analysis of ampicillin in blood. a) Electropherograms for blank blood (bottom) and blood spiked with 2.5 $\mu g\,mL^{-1}$ ampicillin (top). b) The linear calibration curve for ampicillin in blood. Applied voltage for extraction was −100, −500, −100, and +200 (100 s) and for separation was −60, +60, +2200, and −60 for reservoirs 1–4, respectively.

the waste V channel. A fluorescence microscope was used to visualize the behavior of the SMT and a photomultiplier tube was used to measure the fluorescence intensity. For the determination of the ampicillin level, blood samples from a healthy volunteer were spiked to obtain different concentrations (2.5–20.0 $\mu g\,mL^{-1}$). More details are provided in the Supporting Information.

Keywords: antibiotics · dielectric breakdown · electrokinetic trapping · electrophoresis · microfluidics

How to cite: *Angew. Chem. Int. Ed.* **2015**, *54*, 7359–7362
Angew. Chem. **2015**, *127*, 7467–7470

[1] E. L. Fernández, L. Parés, I. Ajuria, F. Bandres, B. Castanyer, F. Campos, C. Farré, L. Pou, J. MariaQueraltó, J. To-Figueras, *Clin. Chem. Lab. Med.* **2010**, *48*, 437–446.
[2] C. Hiemke, P. Baumann, N. Bergemann, A. Conca, O. Dietmaier, K. Egberts, M. Fric, M. Gerlach, C. Greiner, G. Gründer, E. Haen, U. Havemann-Reinecke, E. Jaquenoud Sirot, H. Kirchherr, G. Laux, U. C. Lutz, T. Messer, M. J. Müller, B. Pfuhlmann, B. Rambeck, P. Riederer, B. Schoppek, J. Stingl, M. Uhr, S. Ulrich, R. Waschgler, G. Zernig, *Pharmacopsychiatry* **2011**, *44*, 195–235.
[3] a) F. Pea, P. Viale, *Crit. Care* **2009**, *13*, 214; b) J. A. Roberts, M. Ulldemolins, M. S. Roberts, B. McWhinney, J. Ungerer, D. L. Paterson, J. Lipman, *Int. J. Antimicrob. Agents* **2010**, *36*, 332–339; c) B. M. Patel, J. Paratz, N. C. See, M. J. Muller, M. Rudd, D. Paterson, S. E. Briscoe, J. Ungerer, B. C. McWhinney, J. Lipman, J. A. Roberts, *Ther. Drug Monit.* **2012**, *34*, 160–164; d) S. I. Blot, F. Pea, J. Lipman, *Adv. Drug Delivery Rev.* **2014**, *77*, 3–11.
[4] a) J. H. Beumer, *Clin. Pharmacol. Ther.* **2013**, *93*, 228–230; b) A. Paci, G. Veal, C. Bardin, D. Levêque, N. Widmer, J. Beijnen, A. Astier, E. Chatelut, *Eur. J. Cancer* **2014**, *50*, 2010–2019; c) C. Bardin, G. Veal, A. Paci, E. Chatelut, A. Astier, D. Leveque, N. Widmer, J. Beijnen, *Eur. J. Cancer* **2014**, *50*, 2005–2009.
[5] Y. Le Meur, M. Büchler, A. Thierry, S. Caillard, F. Villemain, S. Lavaud, I. Etienne, P. F. Westeel, B. H. De Ligny, L. Rostaing, E. Thervet, J. C. Szelag, J. P. Rérolle, A. Rousseau, G. Touchard, P. Marquet, *Am. J. Transplant.* **2007**, *7*, 2496–2503.
[6] W. E. Winter, L. J. Sokoll, I. Jialal, *Handbook of diagnostic endocrinology*, AACC Press, Washington, DC, **2008**.
[7] Y. Xiang, Y. Lu, *Nat. Chem.* **2011**, *3*, 697–703.
[8] E. X. Vrouwe, R. Luttge, I. Vermes, A. van den Berg, *Clin. Chem.* **2007**, *53*, 117–123.
[9] Z. Long, D. Liu, N. Ye, J. Qin, B. Lin, *Electrophoresis* **2006**, *27*, 4927–4934.
[10] J. E. Adaway, B. G. Keevil, *J. Chromatogr. B* **2012**, *883–884*, 33–49.
[11] Y.-C. Wang, J. Han, *Lab Chip* **2008**, *8*, 392–394.
[12] J. H. Lee, S. Chung, S. J. Kim, J. Han, *Anal. Chem.* **2007**, *79*, 6868–6873.
[13] A. I. Shallan, A. J. Gaudry, R. M. Guijt, M. C. Breadmore, *Chem. Commun.* **2013**, *49*, 2816–2818.
[14] J. C. McDonald, S. J. Metallo, G. M. Whitesides, *Anal. Chem.* **2001**, *73*, 5645–5650.
[15] H. Kwok, K. Briggs, V. Tabard-Cossa, *PLOS one* **2014**, *9*, e92880.
[16] S. Blot, J. Lipman, D. M. Roberts, J. A. Roberts, *Diagn. Microbiol. Infect. Dis.* **2014**, *79*, 77–84.
[17] *World Sepsis Day.* **2013** [cited 4/2/2014] available from: http://www.world-sepsis-day.org.
[18] a) A. Kumar, D. Roberts, K. E. Wood, B. Light, J. E. Parrillo, S. Sharma, R. Suppes, D. Feinstein, S. Zanotti, L. Taiberg, D. Gurka, A. Kumar, M. Cheang, *Crit. Care Med.* **2006**, *34*, 1589–1596; b) C. McKenzie, *J. Antimicrob. Chemother.* **2011**, *66*, ii25–ii31.
[19] J. H. Requejo, J. Bryce, A. J. Barros, P. Berman, Z. Bhutta, M. Chopra, B. Daelmans, A. de Francisco, J. Lawn, B. Maliqi, E. Mason, H. Newby, C. Presern, A. Starrs, C. G. Victora, *Lancet* **2014**, DOI: 10.1016/S0140-6736(14)60925-9.
[20] G. Wong, A. Brinkman, R. J. Benefield, M. Carlier, J. J. De Waele, N. El Helali, O. Frey, S. Harbarth, A. Huttner, B. McWhinney, B. Misset, F. Pea, J. Preisenberger, M. S. Roberts, T. A. Robertson, A. Roehr, F. B. Sime, F. S. Taccone, J. P. J. Ungerer, J. Lipman, J. A. Roberts, *J. Antimicrob. Chemother.* **2014**, *69*, 1416–1423.
[21] G. Wong, S. Briscoe, S. Adnan, B. McWhinney, J. Ungerer, J. Lipman, J. A. Roberts, *Antimicrob. Agents Chemother.* **2013**, *57*, 6165–6170.
[22] T. G. do Nascimento, E. de Jesus Oliveira, I. D. Basílio Júnior, J. X. de Araújo-Júnior, R. O. Macêdo, *J. Pharm. Biomed. Anal.* **2013**, *73*, 59–64.
[23] S. E. Briscoe, B. C. McWhinney, J. Lipman, J. A. Roberts, J. P. J. Ungerer, *J. Chromatogr. B* **2012**, *907*, 178–184.
[24] G. Koren, *Clin. Chem.* **1997**, *43*, 222–227.

Received: February 25, 2015
Published online: May 4, 2015

